Korean Journal of Chemical Engineering
https://doi.org/10.1007/s11814-024-00214-1

ORIGINAL ARTICLE

Enhanced CO_2 Sequestration Strategy Using CO_2 Capturing Material Synthesized from Spent Railway Tie Concrete

Hyung-Jun Jang[1] · Gyubin Lee[1] · Heeji Yoo[1] · Jae-Young Lee[2] · Hye-Jin Hong[1]

Received: 12 March 2024 / Revised: 20 June 2024 / Accepted: 25 June 2024

Abstract

Lots of railway tie concrete waste are produced which needs appropriate treatment for disposal. This study introduces a novel strategy for converting railway tie concrete waste into a highly efficient CO_2 capturing material (RTC). To enhance the CO_2 capturing capabilities, a $CaCl_2$ solution was employed as a modifying agent (Ca-RTC). The introduction of a 0.001 M $CaCl_2$ solution increased the Ca content in Ca-RTC by only 0.08% compared to unmodified RTC, yet it significantly enhanced porosity and surface area. This modification led to an 11.57% of excellent CO_2 capturing ability, which is 2.5 times greater than that of the original RTC. Even though the Ca content is similar in RTC and Ca-RTC, the significant increase in BET surface area led to a notable improvement in CO_2 capturing ability. However, increasing the $CaCl_2$ concentration beyond 0.005 M resulted in a reduction of CO_2 capturing ability, attributed to the inhibitory effect of Cl^- ions. The kinetics of the CO_2 capturing reaction and the impact of CO_2 pressure on Ca-RTC were systematically investigated. Finally, the CO_2 capturing mechanism of Ca-RTC was elucidated.

Keywords Railway tie concrete · Modification · CO_2 capture · Mineral carbonization

Introduction

In recent years, rapid industrialization has led to climate change, contributing to an increase in unexpected natural disasters worldwide. Among greenhouse gases, carbon dioxide (CO_2) is a primary concern, with its atmospheric concentration nearing 400 ppm and an annual growth rate of approximately 2 ppm since 2000 [1]. The 2015 Paris Agreement underscored the urgency of addressing climate change, setting a global target to limit the average temperature rise to well below 2 °C above pre-industrial levels, and aiming for a cap of 1.5 °C. In response, achieving carbon neutrality has emerged as a universal objective, with nations and organizations around the globe, including the South Korean government, committing to carbon neutrality by 2050 [2].

One of the strategies to mitigate CO_2 emissions involves post-treatment, its capture and conversion into valuable products, such as synthetic fuels [3], chemicals [4] and polymers [5] , or into thermodynamically stable forms like carbonate minerals for long-term sequestration [6]. Among these methods, mineral carbonization, which converts CO_2 into solid minerals, stands out for its simplicity, stability, and the widespread availability of necessary minerals. This process involves the reaction of alkaline earth metal ions, such as calcium (Ca) and magnesium (Mg), with CO_2 gas to form stable compounds like $CaCO_3$ or $MgCO_3$. Given the abundant presence of alkaline earth metals in industrial waste materials—including waste concrete [7, 8], steelmaking slags [9], fly ash [10], incineration ash [11] and cement kiln dust [12]—there has been significant interest in utilizing these materials for CO_2 capture through mineral carbonization.

As of September 2023, 445,652 waste railway concrete ties have been left untreated and abandoned in South Korea. The disposal of these used railway ties poses a critical environmental challenge, necessitating efficient waste

✉ Jae-Young Lee
iyoung@krri.re.kr

✉ Hye-Jin Hong
hyejiny@chungbuk.ac.kr

[1] Department of Environmental Engineering, Chungbuk National University, Chungdae-Ro 1, Seowon-Gu, Cheongju 28644, Chungbuk, Republic of Korea

[2] Transportation Environmental Research Department, Korea Railroad Research Institute (KRRI), #176, Cheoldobangmulgwan-Ro, Uiwang, Geyonggi, Republic of Korea

Published online: 19 July 2024

management strategies to address the disposal of this vast quantity of spent railway ties. Interestingly, these waste railway concrete ties contain approximately 10% alkaline earth metal ions, making them potential candidates for CO_2 capture through mineral carbonation. Our prior research has demonstrated that, although railway ties have a lower content of Ca and Mg compared to regular concrete, they exhibit a CO_2 capture capacity (4.31% CO_2 loading ability) comparable to conventional concrete waste [13]. This is attributed to a high proportion of uncarbonized alkaline earth metals, underscoring their potential as a material for CO_2 capture.

This study aims to augment the CO_2 capture efficiency of waste concrete railway ties by treating them with a $CaCl_2$ solution. Incorporating Ca or Mg sources into materials to enhance their CO_2 capturing capabilities is a widely recognized method, typically involving the use of CaO or MgO) [14, 15]. However, the conventional production of CaO through the calcination of natural limestone inevitably releases a substantial amount of CO_2 [16]. In contrast, $CaCl_2$ can be sourced from seawater or brines, which are abundant natural mineral sources that do not contribute to CO_2 production. Therefore, we explored a novel modification technique to improve the CO_2 capturing ability of spent railway tie concretes, leveraging the environmental benefits of using $CaCl_2$ derived from natural sources.

Initially, we developed a cube-shaped CO_2 capturing material from waste railway tie concrete (RTC) and subsequently modified it with varying concentrations of $CaCl_2$ solution to produce Ca-RTCs. We examined the characteristics of both RTC and Ca-RTCs to understand the modifications induced by the addition of $CaCl_2$. Furthermore, the CO_2 capturing performance of Ca-RTCs was assessed based on the varying amounts of $CaCl_2$ incorporated. We also conducted studies on the kinetics of CO_2 capture and the impact of CO_2 pressure on the capturing efficiency of Ca-RTC, demonstrating the potential of Ca-RTCs as effective CO_2 capturing materials. Finally, we explored the changes in the physicochemical properties of Ca-RTCs post-CO_2 capture to elucidate the mechanism of CO_2 capture by Ca-RTCs.

Materials and Methods

Synthetic Procedure of RTC and Ca-RTC

Railroad tie concrete sourced from Gyeonggi, South Korea, was utilized as the primary material for this study. This concrete was processed into a fine powder by ball milling with tungsten carbide (WC) balls in a stainless steel (SUS) milling jar, operating at 250 rpm for a duration of 12 h. A paste was then produced from the powdered railroad tie concrete by adding a calcium chloride ($CaCl_2$, 97% purity, Sigma–Aldrich) solution in concentrations ranging from 0.0001 to 0.5 M, maintaining a waste-to-solution ratio of 0.45 (w/w). Specifically, 9 mL of the desired concentration of $CaCl_2$ solution was mixed with 20 g of railroad tie concrete powder by hand mixing. The resultant slurry was injected into a 1 cm^3 cubic mold using a 10 mL syringe and dried at 60 °C for 3 days in an oven, resulting in a material designated as Ca-RTC. Ten Ca-RTC cubes were prepared from the slurry. For the synthesis of Ca-RTC, a relatively high temperature of 60 °C was employed to expedite the synthesis of the CO_2 capturing material. Despite this elevated temperature, the carbon (C) content in Ca-RTC was only 1.49%, indicating that the majority of the Ca (10.1%) remained in an uncarbonated form. The added amounts of Ca and Cl (mmol per Ca-RTC cube) are described in table s1.

For comparative purposes, CO_2 capturing materials were also prepared using deionized water (DI water) and a 0.01 M sodium chloride (NaCl, 99% purity, SAMCHUN) solution, labeled as RTC and Na-RTC, respectively. These materials underwent a CO_2 capture experiment following a 3-day hydration process. The preparation process for the CO_2 capturing materials is detailed in Fig. 1.

Characterization of the Ca-RTC Before and After CO_2 Capture

The crystal structures of RTC and Ca-RTC were analyzed using X-ray Diffractometry (XRD, Rigaku, Smartlab). X-ray Fluorescence (XRF, Rigaku, ZSX Primus-II) was employed

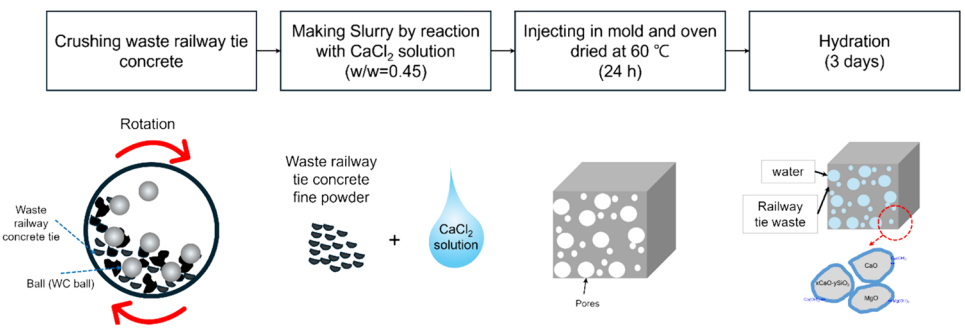

Fig. 1 Schematic draw of Ca-RTC preparation procedure

to investigate their elemental composition and content. The surface area and pore size distribution were measured using Brunauer–Emmett–Teller analysis (BET, Micromeritics, ASAP2020). The BET model is used for determining surface area of Ca-RTC, and BJH (Barrett–Joyner–Halenda) model was used for analysis of pore size distribution. Field Emission Scanning Electron Microscopy (FESEM, Zeiss, Ultra Plus) was used to observe the surface morphology of RTC and Ca-RTC, both before and after the CO_2 capture reaction. Additionally, the elemental distribution of Ca-RTC before and after the CO_2 capture reaction was analyzed by SEM equipped with an Energy Dispersive X-ray Spectrometer (EDAX, Zeiss, Ultim Extreme). The zeta potential of Ca-RTC was measured using a zeta analyzer (Otsuka, ELS-Z) after grinding it into a powder. The alkalinity of Ca-RTC was determined using the following procedure: First, 5 g of ground Ca-RTC were thoroughly mixed with 50 ml of deionized water for 5 min using a vortex mixer. The mixture was then allowed to settle for 20 min. Finally, the pH of the supernatant was measured with a pH meter [17]. Phenolphthalein analysis was conducted to observe reaction kinetics after CO_2 capture; a 1% Phenolphthalein solution (1% Purity, Daejung) was sprayed on freshly cut surfaces, indicating carbonated regions as colorless (pH < 9.2) and non-carbonated regions as purple (pH > 9.2) [18].

CO_2 Capturing Experiments

To evaluate CO_2 capturing abilities of prepared material, one piece (1 cm^3) of CO_2 capturing material was put it to the CO_2 capturing reaction chamber (RAMT, maximum pressure 1 bar, diameter = 22 cm, depth = 50 cm) and evacuation to − 0.5 bar using vacuum pump to remove unwanted molecule bound on CO_2 capturing materials. After 30 min evacuation, a 99.5% CO_2 gas (99.5%, Sejong Industry Gas) atmosphere at a pressure of 0.5 bar for 7 days. To evaluate amount of captured CO_2 on Ca-RTC, thermogravimetric Analysis (TGA, Scinco M&T, TGA N1000) was carried out. The weight change of Ca-RTC was monitored from 25 to 900 °C at a rate of 10 °C/min. Considering the decomposition of $CaCO_3$ between 600 and 900 °C, the formula for calculating the CO_2 absorption capacity is as follows [19]:

$$\text{CaCO}_3 \text{ formedduring CO}_2 \text{ capture reaction}(\%) = \frac{\Delta w_1 - \Delta w_2}{\text{Weight of 900 }^{\circ}\text{C}} \times \frac{100}{43.66}, \quad (1)$$

where Δw_1 and Δw_2 (g) is the weight difference of Ca-RTC at 25 and 900 ℃, after and before CO_2 capturing reaction, respectively. We analyze the TGA of pure $CaCO_3$ to confirm the reliability of $CaCO_3$ decomposition at 900 ℃ and it is discovered that not all $CaCO_3$ was decomposed at 900 ℃ and only 66.3% of weight loss occurred (Fig. S1, see supporting information). Considering this 100/43.66 was multiplied to compensate the actual $CaCO_3$ (%). The CO_2 loading on Ca-RTC was calculated by following equation, by considering molecular weight of CO_2 (44.01 g/mol) and $CaCO_3$(100.1 g/mol), respectively.

$$\text{CO}_2 \text{ loading}(\%) = \text{CaCO}_3 \times \frac{44.01}{100.1}. \quad (2)$$

Results and Discussion

Characterization of RTC and Ca-RTC

Table 1 outlines the compositions of RTC and Ca-RTC. Both materials predominantly consist of silicon (Si), a fundamental component of concrete, with Si compositions of 26.6% and 25.3%, respectively. Following Si, calcium (Ca) is the next most abundant element, playing a crucial role in CO_2 capture reactions, with both RTC and Ca-RTC containing approximately 10% Ca. The inclusion of $CaCl_2$ solution marginally increased the Ca content in the CO_2 capturing materials from 9.82 to 10.10%.

The carbon (C) content in both RTC and Ca-RTC was relatively low, recorded at 0.99% and 1.49% respectively, indicating a minimal presence of CO_2 in their original chemical structures. This suggests that a significant portion of Ca and Mg within the materials remains uncarbonated and available for CO_2 capture reactions. Additionally, other elements such as aluminum (Al), sodium (Na), and iron (Fe) experienced negligible changes, within 0.28%, even after the $CaCl_2$ treatment. Based on the amounts of Ca and Mg, we can estimate the theoretical CO_2 capturing ability of RTC and Ca-RTC. Alkaline earth metals such as Mg and Ca form insoluble mineral carbonates by reacting with CO_2 through the following equations:

$$Ca^{2+} + CO_2 + H_2O \rightarrow CaCO_3 \downarrow,$$

Table 1 Compositions of CO_2 adsorbed prepared by RTC, Ca-RTC

	C	O	Na	Mg	Al	Si	K	Ca	Fe	Others
RTC	0.99	51.8	0.48	0.22	4.4	26.6	2.45	9.82	1.72	1.52
Ca-RTC	1.49	51.3	0.7	0.32	4.4	25.3	2.59	10.10	1.98	1.82

$Mg^{2+} + CO_2 + H_2O \rightarrow MgCO_3 \downarrow$.

Considering that 1 mol of Ca or Mg reacts with 1 mol of CO_2, the theoretical CO_2 capturing ability of Ca-RTC is estimated to be 11.66%.

Figure 2a shows the X-ray diffractometry (XRD) results for RTC and Ca-RTC. Both materials displayed a dominant peak for SiO_2, confirming the predominance of Si in the form of SiO_2 crystals. Despite the low intensity of the $CaCO_3$ peak, it verified the presence of trace crystalline $CaCO_3$. The XRD patterns for RTC and Ca-RTC were similar, indicating that Ca addition did not alter the crystalline structure of the CO_2 capture material. However, differences in morphology between RTC and Ca-RTC were evident in their scanning electron microscopy (SEM) images (Fig. 2e, f). The SEM image for RTC showed relatively smooth surfaces, whereas Ca-RTC exhibited large pores ranging from 10 to 100 µm and small aggregates, affecting the specific surface area as demonstrated in the nitrogen adsorption–desorption isotherms in Fig. 2b. Compared with raw railway tie concrete (before crushing), the crushing and reconstruction of Ca-RTC (or RTC) into a 1 cm^3 cube structure significantly affects its morphology. The raw railway tie concrete exhibits a flat and non-porous surface, which hinders the reaction of alkaline earth metals (Ca or Mg) in concrete waste and results in relatively prolonged carbonation

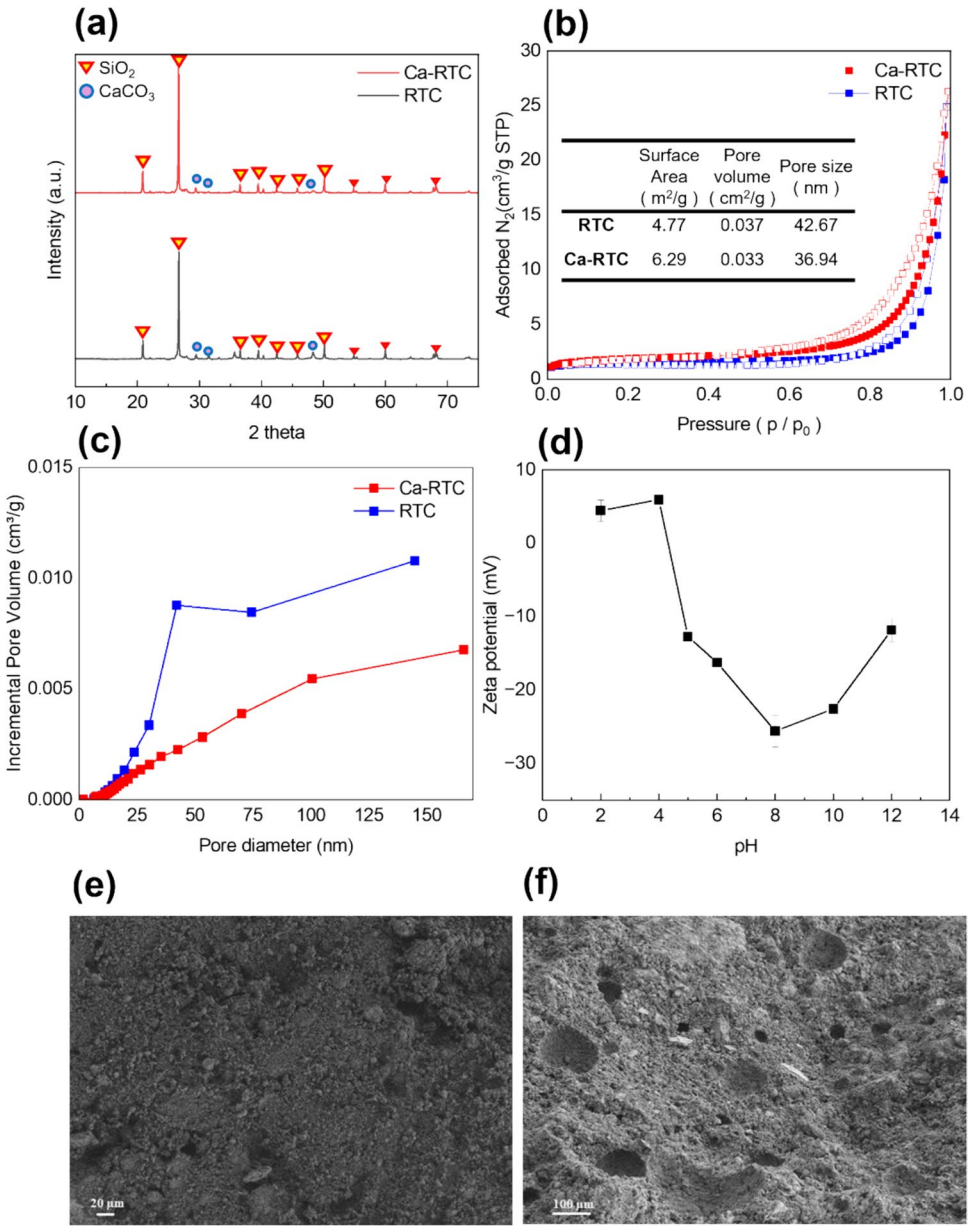

Fig. 2 XRD patterns (**a**), N_2 adsorption–desorption isotherm (**b**), pore size distribution (**c**), zeta potential (**d**) of RTC and Ca-RTC, and SEM images of RTC (**e**) and Ca-RTC (**f**)

kinetics (Fig. S2). In contrast, both RTC and Ca-RTC exhibit hysteresis loops indicative of mesoporous materials. Notably, Ca-RTC has a higher specific surface area of 6.29 m^2/g, approximately 1.52 m^2/g greater than that of RTC (4.77 m^2/g). The pore structure analysis indicated a reduction. In total pore volume but an Increase In average pore size from 36.9 to 42.7 nm after Ca addition, suggesting that the surface area increase is attributed to the formation of numerous particles rather than an increase in mesopore size (Fig. 2c).

The formation of these pores likely occurs during Ca-RTC fabrication, where Ca is introduced as a $CaCl_2$ solution. This process involves the hydration and ionization of $CaCl_2$, producing Ca^{2+} and Cl^- ions that adhere to the RTC particle surfaces, making them more hydrophilic. Consequently, more H_2O molecules are attracted to the surface of Ca-RTC due to its increased hydrophilicity compared to RTC. Upon oven drying, the water is removed, resulting in the formation of smaller aggregates on the surface of Ca-RTC than on RTC. This expanded surface area is anticipated to enhance the CO_2 capturing capability of the material. We also analyzed the zeta potential of Ca-RTC as a function of solution pH (Fig. 2d). At pH levels between 2 and 4, Ca-RTC exhibited a slightly positive charge of approximately 5 mV. However, as the solution pH increased, the zeta potential decreased significantly, becoming negative. At pH 8, a markedly negative zeta potential of − 30 mV was observed. Considering that the pH of hydration water ranges from 5 to 6, Ca-RTC exhibited a negative zeta potential of − 20 mV within this range. During hydration, fewer Ca^{2+} ions are released from the Ca-RTC surface due to electrostatic interactions compared to Cl^- ions. Additionally, we measured the alkalinity of Ca-RTC, which was found to be 12.87, indicating significant potential as a CO_2 capturing material.

CO_2 Capturing Behavior by Ca-RTC

To investigate the effect of $CaCl_2$ concentration on CO_2 capture, experiments were conducted with Ca-RTCs prepared at various $CaCl_2$ concentrations (Fig. 3a). After seven days of CO_2 capture experiments, the pristine RTC showed a CO_2 loading capacity of 4.35%. By adding 0.0001–0.5 M $CaCl_2$ solution to preparation of Ca-RTC, the CO_2 capturing ability is significantly enhanced. By increasing $CaCl_2$ concentration from 0.0001 to 0.001 M, the CO_2 capturing ability is proportionally increased and Ca-RTC with 0.001 M $CaCl_2$ concentration shows 11.57%, which more than doubles the capacity compared to the untreated RTC. However, further increase of $CaCl_2$ concentration caused decrease of CO_2 capturing ability. Even though Ca content in Ca-RTC is increased by increasing $CaCl_2$ concentration, the highest CO_2 capturing performance was obtained with not 0.5 M $CaCl_2$ concentration, but 0.001 M of lower $CaCl_2$ concentration. If the enhancement were solely due to the Ca added in the Ca-RTCs, the CO_2 loading capacity should increase proportionally with $CaCl_2$ concentration. However, the 0.001 M $CaCl_2$ solution, which is the middle range of $CaCl_2$ concentration resulted in the highest CO_2 loading capacity. Additionally, the Ca content in the Ca-RTC prepared with the 0.001 M $CaCl_2$ solution is 10.1%, which is only a 0.28% increase compared to RTC. This result indicates that the extra Ca supplied by the $CaCl_2$ solution is not the reason for the enhanced CO_2 capturing ability. It is expected that the increase in CO_2 capturing ability is due to the increased BET surface area, as discussed in Sect. 1.

To further validate this point, Na-modified RTC (Na-RTC) was produced by adding Na ions, which do not participate in the mineral carbonation reaction, and its CO_2 capture performance was evaluated (Fig. 3a). Na-RTC exhibited a CO_2 loading capacity of 7.73%, which is 3.38% higher than that of RTC even though its alkaline earth metal (Ca and Mg) content is similar to pristine RTC.

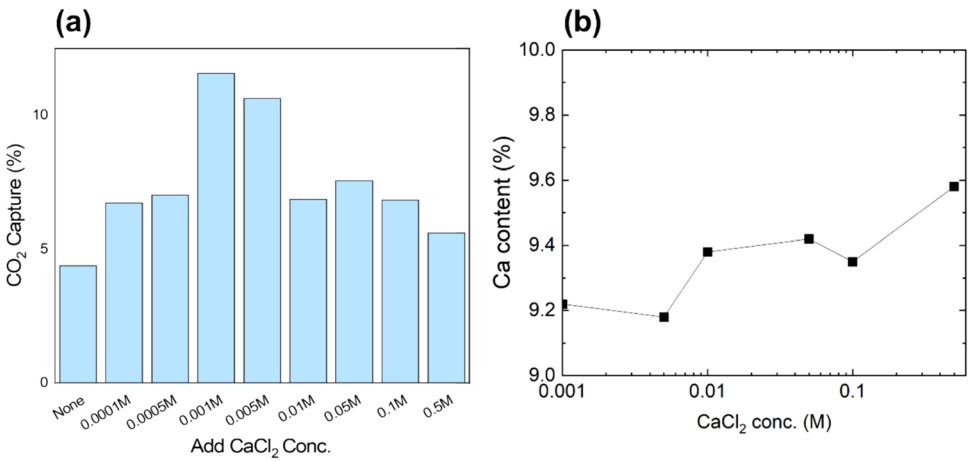

Fig. 3 CO_2 capturing abilities (**a**) and Ca content (%) (**b**) of Ca-RTCs by $CaCl_2$ solution concentration

This result clearly proved that the enhanced CO_2 loading capacity of Ca-RTC was not solely caused by addition of Ca into the material. Moreover, like Ca-RTC, Na-RTC showed an increased specific surface area of 5.78 m^2/g compared to RTC, and its surface morphology became similar to that of Ca-RTC (refer to Fig. S3). The increase in CO_2 capturing capacity due to the addition of Na ions is attributed to the expanded surface area, as Na ions do not participate in the CO_2 loading reaction. In RTC, the Ca ions originally present were not completely reactive with CO_2 within 7 days due to relatively low porosity and blocking. However, the expansion of surface area resulting from the addition of Na ions facilitates the reaction between Ca and CO_2, thereby increasing the CO_2 sorption capacity. These findings suggest that the surface area and pore structure of CO_2 capture materials are significantly affected by ionic strength during the manufacturing process, with an increase in ion concentration in the composite leading to an enlarged specific surface area.

However, a further increase in $CaCl_2$ concentration did not result in a higher CO_2 capture ability (Fig. 3a). Analysis of the Ca content in Ca-RTCs prepared with different $CaCl_2$ concentrations (Fig. 3b) showed a slight increase in Ca content from 9.22 to 9.58% with increased $CaCl_2$ concentration. This indicates that the CO_2 capture ability is not solely dependent on the Ca or Mg content within the Ca-RTCs, despite Ca being a critical ion for the mineral carbonation reaction. The decreased trend in CO_2 capturing ability with increasing $CaCl_2$ concentration is not fully understood, but it is thought to be due to the inhibitory effect of Cl^- ions on the mineral carbonation reaction. As the concentration of $CaCl_2$ increases, so does the concentration of Cl^- ions, which has been reported to significantly reduce the rate of mineral carbonation on lime mud surfaces. Specifically, a Cl:Ca ion ratio greater than 2:100 has been shown to dramatically reduce CO_2 capturing ability [20] . We also analyze the Cl:Ca ratio of Ca-RTC prepared at 0.5 M $CaCl_2$ solution. The Cl:Ca ratio was 2.57:100, which can affect the CO_2 capturing ability.

Following up, CO_2 capture experiments were carried out with Ca-RTC treated with 0.001 M $CaCl_2$ solution. Figure 4a illustrates the kinetics of CO_2 capture by Ca-RTC. Upon injecting 99% CO_2 at 0.5 bar, the CO_2 loading rate surged to approximately 6% after just one day of capture, climbing to 10% after 3 days, and eventually reaching the saturation point of CO_2 capture capacity. Given the initial Mg and Ca content in Ca-RTC (refer to Table 1), it is deduced that Ca-RTC achieved its theoretical maximum CO_2 capture capacity. When examining the phenolphthalein response inside the CO_2 capture material at various stages of capture, samples pre-capture and post one day of capture exhibited a pink color, signaling incomplete carbonate reactions due to the interaction with residual alkaline earth metals. However, samples taken after three days of reaction maintained their colorless state upon applying the same indicator, signifying the completion of the carbonate reaction. Although the carbonate reaction rate was anticipated to be influenced by CO_2 diffusion into the Ca-RTC's interior macropores, the observed rapid penetration of CO_2, attributable to the material's high porosity and extensive specific surface area, indicated a quicker internal reach than expected.

We compared the CO_2 capturing abilities of industrial waste-derived CO_2 capture materials with Ca-RTC (Table 2). Except for magnesium slag, which contains more than 50% high CaO content, Ca-RTC demonstrates the highest CO_2 capturing ability. Despite its relatively low Ca content of 15.0%, compared to other industrial wastes, Ca-RTC exhibits excellent CO_2 capturing performance. This result indicates that Ca-RTC is a highly reliable and effective CO_2 capturing material, emphasizing the reactivity of Ca for carbonation by increasing the surface area of the CO_2 capturing material.

To identify the rate-limiting step in CO_2 capture, both the pseudo-second-order reaction kinetic model and the intraparticle diffusion model were employed (see

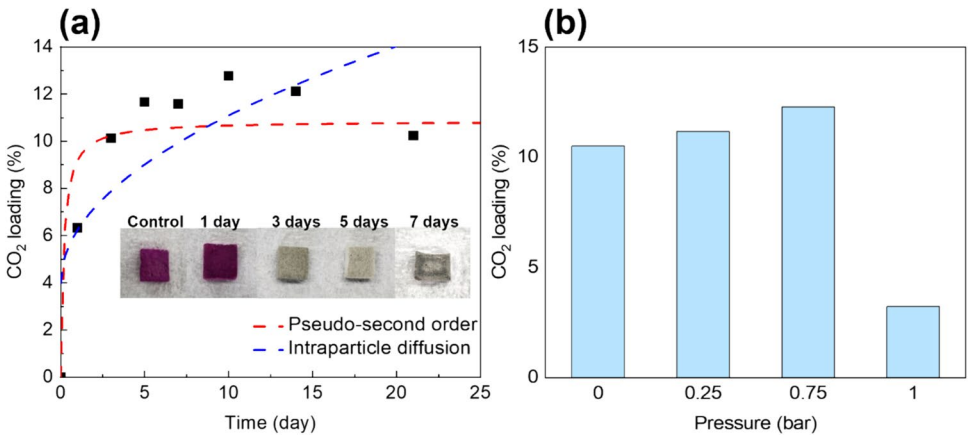

Fig. 4 CO_2 loading on Ca-RTC as a function of reaction time. Inset: phenolphthalein analysis of Ca-RTC (**a**) and CO_2 loading on Ca-RTC under various pressure (**b**)

Table 2 CO_2 capturing abilities of industrial waste and Ca-RTC

	Raw material	Carbonation time (d)	Hydration	CO_2 capturing ability (%)	Ca and Mg content (%)		References
					CaO	MgO	
RTC	Railway tie concrete	7	O	4.31	15.6	0.381	This study
Ca-RTC	Railway tie concrete	10	O	12.76	15.9	0.576	This study
Cement Kiln dust	Alkaline wastes	28	–	4	61.15	3.84	[18]
Magnesium slag	Industrial byproduct	14	O	15.6	53.86	7.24	[19]
Coal fly ash	Burning of pulverized coal	28	–	0.52	22.75	4.48	[18]
Glass powder	Industrial byproduct	28	–	2.49	9.70	3.30	[18]

supporting information). We expressed amount of CO_2 captured on Ca-RTC as mg CO_2 per g Ca-RTC in Fig. 4a and described kinetic model constants in table S2. While the intraparticle diffusion model yielded a linear regression coefficient of merely 0.60, the pseudo-second-order model demonstrated an excellent fit with a linear regression coefficient (R^2) of 0.98. This suggests that CO_2 diffusion into Ca-RTC was notably rapid, and the chemical reaction between CO_2 and the alkaline earth metals within Ca-RTC constituted the rate-limiting step of the overall reaction. The maximum CO_2 capturing amount expected from pseudo-second order model kinetic model was described as 142.85 mg/g (=CO_2 loading 14.28%) which is similar and even higher than theoretical CO_2 capturing capacity of Ca-RTC.

To further explore the impact of pressure on CO_2 capture by Ca-RTC, experiments were conducted over a 1-day period at pressures of 0, 0.25, 0.75, and 1 bar, as shown in Fig. 4b. Given that CO_2 capture reached saturation after 3 days at 0.5 bar, as demonstrated in the kinetics experiment, the efficiency of CO_2 loading in Ca-RTC under varying pressures was assessed over a shorter duration of 1 day. At atmospheric pressure (0 bar), CO_2 loading over the 1-day period was 10.5%. An increase in pressure from 0.25 to 0.75 bar led to higher CO_2 capture rates of 11.17% and 12.28%, respectively. The CO_2 capture at 0.75 bar aligned with the theoretical adsorption capacity of Ca-RTC, suggesting that a pressure increase up to 0.75 bar positively influences the mineral carbonation reaction. This enhancement in the mineral carbonation reaction at approximately 0.75 bar is attributed to the high pressure, which, according to previous kinetic experiments, does not significantly affect the diffusion rate of CO_2 due to Ca-RTC's large surface area. Thus, the observed increase in CO_2 capture rate with pressure is primarily due to an accelerated reaction rate of CO_2 mineral carbonation, rather than an increase in diffusion rate. According to Le Chatelier's principle, an increase in pressure shifts the equilibrium to minimize the system's volume. [21] However, a further increase in CO_2 pressure to 1 bar resulted in a sharp decline in CO_2 loading. During the mineral carbonation reaction, water needs to be released from calcium or magnesium hydroxide, as represented by the reactions:

$$Ca(OH)_2 + CO_2(g) \rightarrow CaCO_3(g) + H_2O\,(g), \quad (3)$$

$$Mg(OH)_2 + CO_2(g) \rightarrow MgCO_3(g) + H_2O\,(g). \quad (4)$$

The increased pressure enhances the water retention capability, thereby reducing the mineral carbonation efficiency of Ca-RTC. Feng et al. reported similar findings, noting a decrease in CO_2 capturing ability of $Ca(OH)_2$ as a CO_2 capturing material at pressures higher than 8 MPa [22].

CO_2 Sequestration Mechanism by Ca-RTC

We clarified the mechanism behind CO_2 capture by analyzing the physicochemical properties of Ca-RTC both before and after the CO_2 capture reactions. Notably, the crystallinity of Ca-RTC remained largely unchanged through the process of CO_2 absorption. However, the post-capture X-ray Diffraction (XRD) analysis revealed a marked increase in the intensity of the $CaCO_3$ peak, suggesting the formation of $CaCO_3$ within Ca-RTC via the carbonation of calcium in the presence of CO_2 as the precursor (Fig. 5a). This transformation involves gaseous CO_2 converting into solid $CaCO_3$, a change that was accompanied by a significant increase in the material's specific surface area, as shown in Fig. 5b. Specifically, the specific surface area of Ca-RTC more than doubled, from 6.29 m^2/g before CO_2 capture to 15.94 m^2/g afterwards. Post-capture, there was a notable increase in the volume of macropores larger than 50 nm (Fig. 5c), while the volume of nano and mesopores remained similar to that of the untreated Ca-RTC. Given that $CaCO_3$ is in a solid phase, in contrast to the gaseous phase of its precursor CO_2, this suggests the creation of new surfaces during the carbonation reaction.

We also analyzed the FTIR spectrum of Ca-RTC before and after the CO_2 capturing reaction (Fig. 5d).

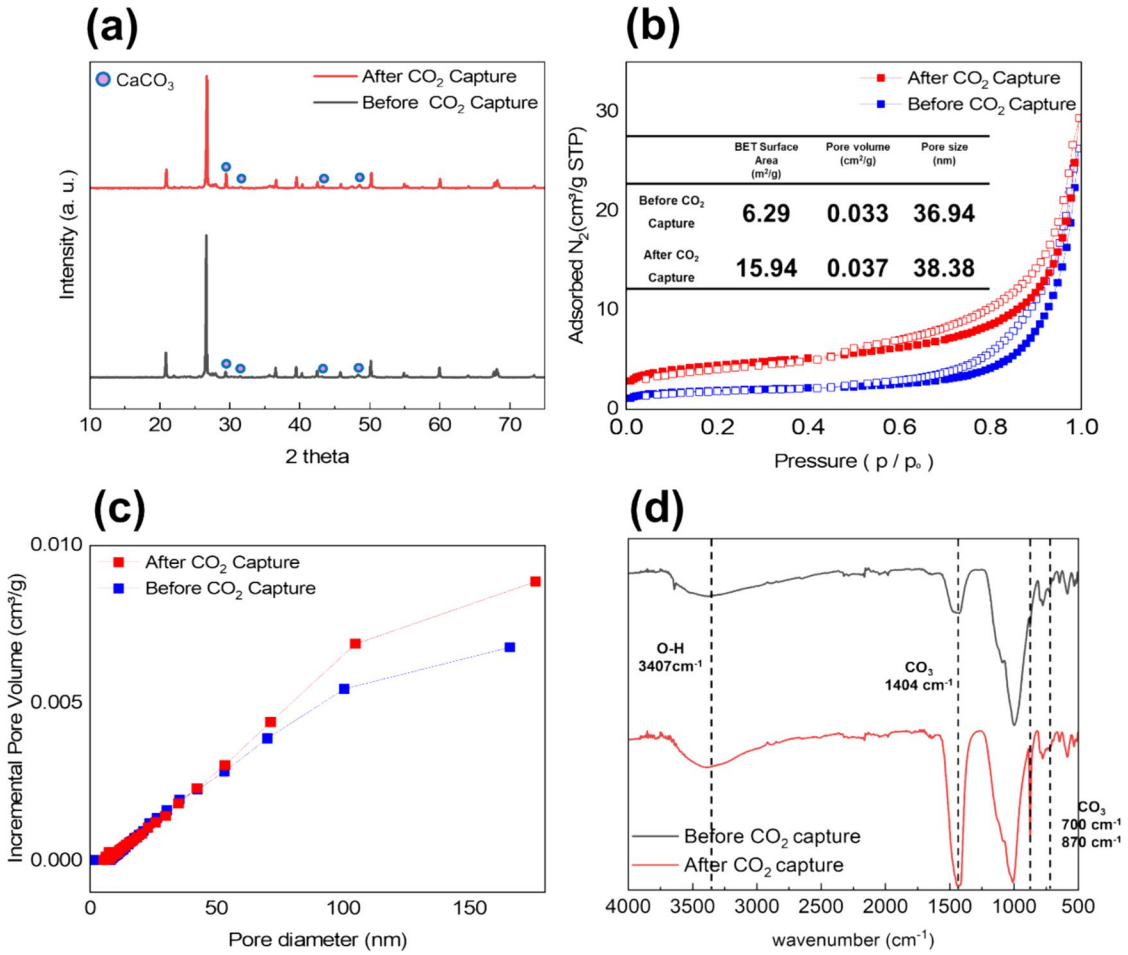

Fig. 5 XRD patterns (**a**), N_2 adsorption–desorption isotherms (**b**), pore size distributions (**c**), and FTIR spectrums (**d**) of Ca-RTC before and after CO_2 capture

The Ca-RTC consists of significant amounts of SiO, and peaks corresponding to Si–O–Si bonds were observed at 1010–1074 cm^{-1} [23] . Additionally, the peak at 3707 cm^{-1}, representing the –OH group, was evident due to the hydration of Ca-RTC. A slight asymmetric CO_3 peak was also observed at 1404 cm^{-1} due to partial carbonation reaction. After the CO_2 capturing reaction, the intensity of peaks at 1404, 870, and 700 cm^{-1}, which represent the peaks of calcite ($CaCO_3$) [24], significantly increased. This result clearly supports that the CO_2 capturing mechanism of Ca-RTC involves the mineral carbonation of Ca ions.

Scanning Electron Microscopy (SEM) analysis post-CO_2 capture revealed the formation of numerous fine particles, less than 1 µm in size, on the surface of Ca-RTC. These particles, which filled the spaces between larger and mesopores, led to a denser structural arrangement (Fig. 6a,b). These newly formed particles are believed to be crystalline $CaCO_3$, as corroborated by the XRD findings. Furthermore, SEM–energy dispersive x-ray analysis (EDAX) imaging of Ca-RTC post-CO_2 capture (Fig. 6c) indicated that $CaCO_3$ did not exist as isolated particles but rather, calcium and carbon were uniformly distributed across the surface of Ca-RTC. Silicon, the predominant component of Ca-RTC, was found to be co-distributed with aluminum, mostly in the form of aluminum silicate and crystalline SiO_2. The areas with a high concentration of silicon and aluminum were distinct from those rich in calcium. The coinciding distributions of carbon with calcium, as previously identified in the XRD analysis, confirmed that CO_2 was converted into $CaCO_3$. This comprehensive evidence supports the conclusion that CO_2 capture in Ca-RTC is directly associated with the formation of $CaCO_3$, effectively elucidating the material's CO_2 capture mechanism.

Conclusion

This study presents an innovative approach to carbon dioxide (CO_2) capture by leveraging modified spent railway tie concrete (RTC), aiming to address the pressing need for

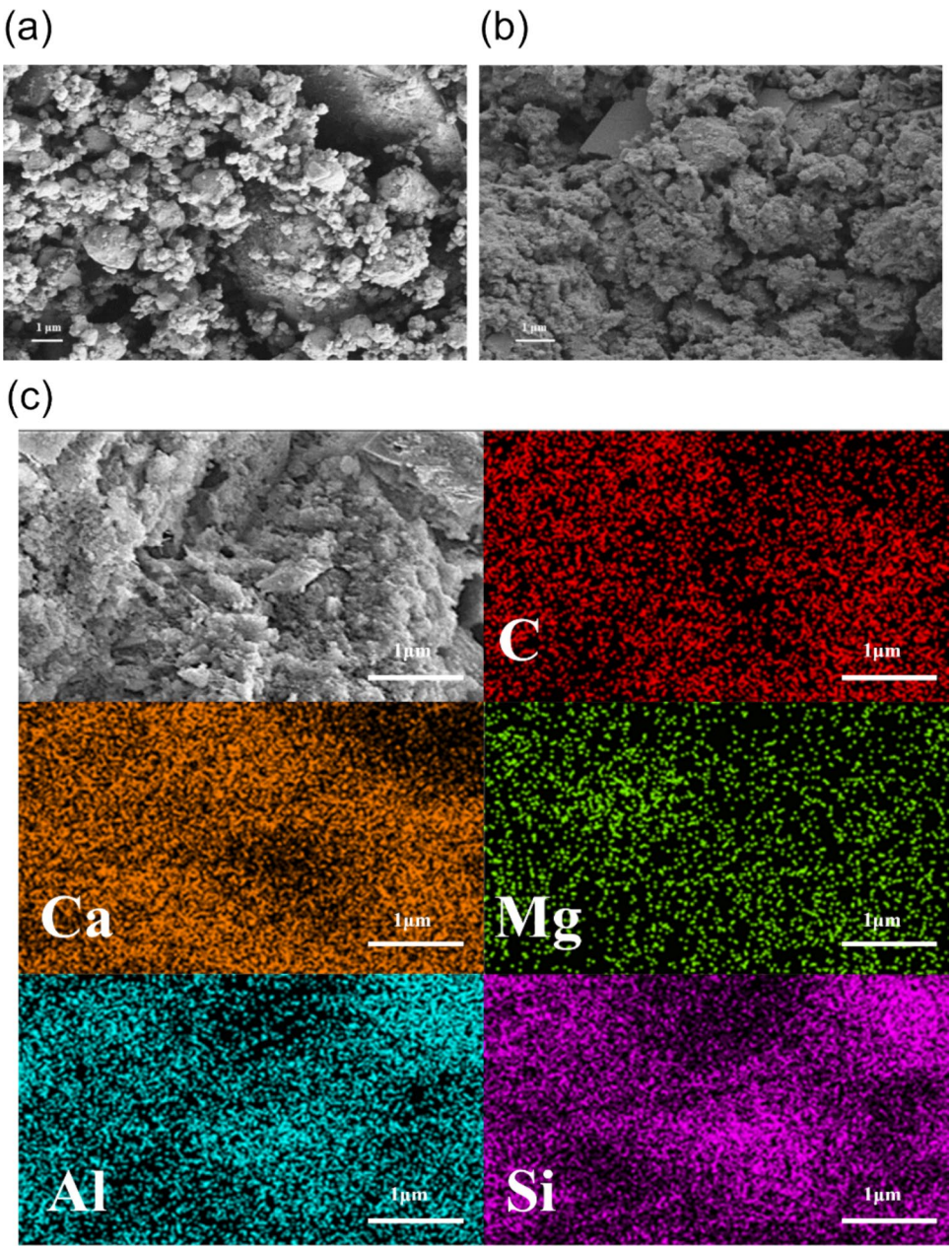

Fig. 6 SEM images of Ca-RTC before (**a**) and after CO_2 capturing (**b**), SEM-EDAX mapping of CO_2 captured Ca-RTC (**c**)

efficient CO_2 sequestration technologies. By incorporating a 0.001 M calcium chloride ($CaCl_2$) solution in lieu of water, we developed a calcium-modified RTC (Ca-RTC) that exhibits a significantly enhanced CO_2 capturing capability. The preparation process involved mixing the waste material with a water/waste ratio of 0.45 (w/w), followed by drying and hydration to form 1 cm^3 cubes. Despite a marginal increase in calcium content (0.08%) compared to the pristine RTC, the Ca-RTC modified with 0.001 M $CaCl_2$ solution demonstrated a substantial increase in BET surface area to 6.29 m^2/g and a highly porous morphology. These changes are attributed to the altered surface properties induced by the ionic strength of the $CaCl_2$ solution, resulting in a 2.5-fold increase in CO_2 capture efficiency (11.57%) over the unmodified RTC. This enhancement is primarily due to the enlarged surface area, facilitating greater CO_2 adsorption. However, increasing the concentration of $CaCl_2$ beyond 0.001 M led to a decrease in CO_2 capturing performance, likely due to the inhibitory effect of Cl^- ions. The CO_2 capture reaction with 0.001 M $CaCl_2$-modified Ca-RTC was completed within three days under 0.5 bar pressure, with the chemical interaction between alkaline earth metal ions in Ca-RTC and CO_2 identified as the rate-limiting step. Furthermore, elevating CO_2 pressure to 0.75 bar enhanced the capture rate, whereas pressures above 1 bar adversely affected the CO_2 capturing ability. Post-reaction analysis

revealed the formation of crystalline calcium carbonate ($CaCO_3$), contributing to an increased surface area of the material. This study not only elucidates the mechanisms underpinning the improved CO_2 capture performance of Ca-RTC but also highlights its potential as a sustainable and efficient solution for CO_2 sequestration.

Supplementary Information The online version contains supplementary material available at https://doi.org/10.1007/s11814-024-00214-1.

Acknowledgements This work was supported by basic research project from Korea Railroad Research Institute (PK2402C2) and Korea Ministry of Environment (MOE) as 'Waste to Energy-Recycling Human Resource Development Project'.

Author Contributions H-JJ: writing—original draft, and investigation. GL: investigation and analysis. HY: formal analysis. J-YL: supervision and conceptualization. H-JH: writing—review and editing, supervision, and conceptualization.

Data availability The datasets used and/or analyzed during the current study are available from the corresponding author on reasonable request.

Declarations

Conflict of Interst The authors declare that they have no known competing financial interests or personal relationships that could have appeared to influence the work reported in this paper.

References

1. W.J.J. Huijgen, R.N.J. Comans, Carbon dioxide sequestration by mineral carbonation. Literature review, IAEA report, 52 p (2003)
2. H. Oh, I. Hong, I. Oh, South Korea's 2050 carbon neutrality policy. East Asian Policy **13**(01), 33–46 (2021)
3. T. Qu, S. Wei, Z. Xiong, J. Zhang, Y. Zhao, Progress and prospect of CO_2 photocatalytic reduction to methanol. Fuel Process. Technol. **251**, 107933 (2023)
4. F. Zhang, Z. Wei, G. Jiang, G. Li, M. Zhao, Z. Zhang, J. Cheng, Z. Hao, Synergistic conversion of acid gases (H_2S and CO_2) to valuable chemicals: carbonyl sulfide synthesis over vacancy-defective CoMo sulfide catalysts. Appl. Catal. B **319**, 121912 (2022)
5. K. Sadeghi, Y. Jeon, J. Seo, Roadmap to the sustainable synthesis of polymers: from the perspective of CO_2 upcycling. Progress Mater. Sci. **135**, 101103 (2023)
6. H. Liu, H. Lu, H. Hu, CO_2 capture and mineral storage: State of the art and future challenges. Renew. Sustain. Energy Rev. **189**, 113908 (2024)
7. H. Liu, Q. Li, Preparation of artificial aggregates from concrete slurry waste and waste brick masonry powder: CO_2 uptake and performance evaluation. Constr. Build. Mater. **382**, 131356 (2023)
8. W.-H. Xie, H. Li, M. Yang, L.-N. He, H.-R. Li, CO_2 capture and utilization with solid waste. Green Chem. Eng. **3**(3), 199–209 (2022)
9. X. Wang, X. Wei, W. Ni, Impacts of hydration degree of steel slag on its subsequent CO_2 capture behaviors and mechanical performances of prepared building materials. Constr. Build. Mater. **416**, 135075 (2024)
10. H. Li, Y. Peng, M. Xu, Y. Wang, J. Ding, B. Ma, L. Jin, S. Lu, J. Yan, Use of municipal solid waste incineration fly ash as a supplementary cementitious material: CO_2 mineralization coupled with mechanochemical pretreatment. Environ. Res. **242**, 117799 (2024)
11. D. Zhang, Y. Zhang, P. Lei, Z. Yang, L. Liu, Z. Zhang, CaO-based adsorbents derived from municipal solid waste incineration bottom ash for CO_2 capture. Sustain. Mater. Technol. **39**, e00856 (2024)
12. S.K. Adekunle, Carbon sequestration potential of cement kiln dust: mechanisms, methodologies, and applications. J. Clean. Prod. **446**, 141283 (2024)
13. G. Lee, J.-Y. Lee, H.-J. Jang, S. Ko, H.-J. Hong, Research on the production of CO_2 absorbent using railway tie concrete waste. J. Korean Recycl. Construct. Resour. Inst. **11**(3), 260–266 (2023)
14. P. Teixeira, C. Bacariza, I. Mohamed, C.I. Pinheiro, Improved performance of modified CaO-Al_2O_3 based pellets for CO_2 capture under realistic Ca-looping conditions. J. CO2 Util. **61**, 102007 (2022)
15. P.C. de Carvalho Pinto, G.V. Pereira, L.S. de Rezende, F.C. Moura, J.C. Belchior, CO_2 capture performance and mechanical properties of $Ca(OH)_2$-based sorbent modified with MgO and (NH_4) $2HPO_4$ for Calcium Looping cycle. Fuel **256**, 115924 (2019)
16. E. Wu, Q. Wang, L. Ke, G. Zhang, Study on carbon emission characteristics and emission reduction measures of lime production—a case of enterprise in the Yangtze River Basin. Sustainability **15**(13), 10185 (2023)
17. F. Björk, C.A. Eriksson, Measurement of alkalinity in concrete by a simple procedure, to investigate transport of alkaline material from the concrete slab to a self-levelling screed. Constr. Build. Mater. **16**(8), 535–542 (2002)
18. D.P. Siriwardena, S. Peethamparan, Quantification of CO_2 sequestration capacity and carbonation rate of alkaline industrial byproducts. Constr. Build. Mater. **91**, 216–224 (2015)
19. L. Mo, Y. Hao, Y. Liu, F. Wang, M. Deng, Preparation of calcium carbonate binders via CO_2 activation of magnesium slag. Cem. Concr. Res. **121**, 81–90 (2019)
20. R. Sun, R. Xiao, J. Ye, Kinetic analysis about the CO_2 capture capacity of lime mud from paper mill in calcium looping process. Energy Sci. Eng. **8**(11), 4014–4024 (2020)
21. B.K. Arumugam, P.C. Wankat, Pressure transients in gas phase adsorptive reactors. Adsorption **4**, 345–354 (1998)
22. Y. Fang, J. Chang, M. Cao, Influence of compaction pressure on the accelerated carbonation of calcium hydroxide. J. Wuhan Univ. Technol. Mater. Sci. Ed. **31**(6), 1187–1192 (2016)
23. L.M. Johnson, L. Gao, C.W. Shields IV., M. Smith, K. Efimenko, K. Cushing, J. Genzer, G.P. López, Elastomeric microparticles for acoustic mediated bioseparations. J. Nanobiotechnol. **11**, 1–8 (2013)
24. J.D. Rodriguez-Blanco, S. Shaw, L.G. Benning, The kinetics and mechanisms of amorphous calcium carbonate (ACC) crystallization to calcite, via vaterite. Nanoscale **3**(1), 265–271 (2011)